Journal of Biomechanics 45 (2012) 2215–2221

Contents lists available at SciVerse ScienceDirect

Journal of Biomechanics

journal homepage: www.elsevier.com/locate/jbiomech
www.JBiomech.com

Computed tomography analysis of knee pose and geometry before and after total knee arthroplasty

K.C.T. Ho [a,b], S.K. Saevarsson [a,b], H. Ramm [c], R. Lieck [c], S. Zachow [c], G.B. Sharma [a,b], E.L. Rex [a,b], S. Amiri [d], B.C.Y. Wu [a], A. Leumann [e], C. Anglin [a,b,f,*]

[a] Biomedical Engineering, University of Calgary, Calgary, Canada
[b] McCaig Institute for Bone and Joint Health, University of Calgary, Calgary, Canada
[c] Zuse Institute Berlin, Berlin, Germany
[d] Department of Orthopaedics, University of British Columbia, Vancouver, Canada
[e] Department of Orthopaedic Surgery, Basel University Hospital, Basel, Switzerland
[f] Department of Civil Engineering, University of Calgary, Calgary, Canada

ARTICLE INFO

Article history:
Accepted 14 June 2012

Keywords:
Total knee arthroplasty
Computed tomography
Pose
Geometry
Patella
3D–3D matching

ABSTRACT

Using a three-dimensional (3D) modality to image patients' knees before and after total knee arthroplasty (TKA) allows researchers and clinicians to evaluate causes of pain after TKA, differences in implant design, and changes in the articular geometry as a result of surgery. Computed tomography (CT) has not been fully utilized to date for evaluating the knee after TKA due to metal artifacts obscuring part of the image. We describe an accurate, validated protocol, which has been implemented in vivo, that improves visibility of the patellofemoral joint, matches implant models automatically in 3D, segments preoperative bone semi-automatically, detects and sets coordinate systems automatically, determines the six degrees of freedom of knee pose and geometry, and allows for multiple other measurements that are clinically relevant. Subjects are imaged at 0° and 30° knee flexion, while pushing on a custom-made knee rig to provide partial loadbearing. With some modifications, the protocol can be adopted by any group with access to a CT scanner and image analysis software, allowing for the investigation of numerous clinical and biomechanical questions.

1. Introduction

Total knee arthroplasty (TKA) is a highly advanced procedure for treating severe knee osteoarthritis, with over 500,000 TKA procedures performed in North America each year (DeFrances et al., 2007). Drawbacks exist, however, with poor surgical technique and implant design leading to pain, prosthesis loosening, patellar maltracking, and other inferior outcomes. Differences between patients with good and poor outcomes, particularly of the patellofemoral (PF) joint, are not clearly understood, and existing in vivo methods to investigate the PF joint are limited.

Three-dimensional (3D) imaging offers the ability to measure the full 6 degrees of freedom (DOF) of the knee (bone or implant) in different positions, and to compare the 3D geometry of patients' knees before and after surgery. CT provides fast, high resolution, three-dimensional knee visualization, permitting accurate measurement of pre-and post-TKA knee pose and geometry. Use of CT for post-TKA assessment has been limited in the past because of metal streak artifacts, even with metal artifact reduction algorithms implemented; however, we have developed methods to mitigate the problem. While radiation has also been a concern, radiation dose at the extremities of older individuals poses relatively low risk, particularly with newer scanner technologies and low-dose protocols (Henckel et al., 2006; Van Sint Jan et al., 2006).

A number of clinically-relevant parameters can be measured from CT including: improper component rotation, patellar maltracking, changes in joint line height and excessive varus or valgus alignment. Improper component rotation can lead to anterior knee pain after TKA; incorrect implant placement can lead to joint overstuffing, mediolateral overhang and instability. 3D models that are derived from CT data can be used for many other purposes as well, including finite element analyses and 2D/3D matching to radiographs.

To date, only manual methods have been used to fit 3D implant models to CT scans (Henckel et al., 2006; Hirschmann et al., 2010) or to segment the prosthesis shape. An automated fitting method should reduce the user time required and make the procedure more repeatable.

The purpose of this study, therefore, was to develop and validate a clinical CT imaging protocol to determine knee pose (i.e. relative position and orientation of the bones or prostheses)

* Corresponding author at: Department of Civil Engineering, University of Calgary, 2500 University Dr. NW, Calgary, AB, T2N 1N4, Canada. Tel.: +1 403 220 7418; fax: +1 403 282 7026.
E-mail address: canglin@ucalgary.ca (C. Anglin).

0021-9290/$ - see front matter © 2012 Elsevier Ltd. All rights reserved.
http://dx.doi.org/10.1016/j.jbiomech.2012.06.004

and geometry such that preoperative and postoperative (pre- and post-) TKA patellofemoral (PF) and tibiofemoral (TF) relative positioning, as well as patellar shift within the femoral groove, and hip–knee–ankle (HKA) alignment can be measured. For the postoperative joint, a further goal of this study was to develop methods to measure PF and TF contact locations, component rotations, joint line height, patellar cut symmetry and patellar height. To our knowledge, this is the first time that CT has been used to investigate knee pose and geometry measures before or after TKA. This protocol can be adopted by anyone with access to a CT scanner and image analysis software.

2. Methods

The image acquisition and image analysis procedures used are described first, followed by the validation and repeatability procedures.

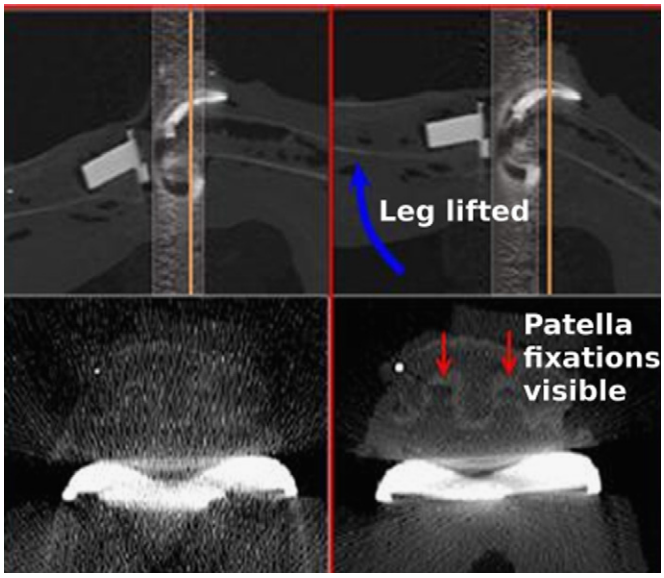

Fig. 1. Raising the leg improves patellar visibility by shifting the metal artifact band (shown in grey), which passes through the thickest portion of the femoral component, more distally on the femoral component. This significantly improves the visibility of the patellar fixations (shown on the bottom).

2.1. Image acquisition

The preop and postop protocols are similar. In both cases, individuals are imaged at 0° and 30° knee flexion, i.e. in full extension, and after the patella engages in the femoral groove. Pilot testing with cadaveric specimens up to 60° flexion revealed that, beyond 30°, patellar visibility becomes unacceptable (Ho, 2010). The central novelty of the procedure relates to the postop protocol: for the TKA subjects, the foot is raised using a custom knee rig such that the metal artifact from the femoral component obscures less of the patellar bone and component than when the foot is not raised (Fig. 1). The metal artifact band passes through the thickest part of the femoral component in the plane of the CT bore; by tilting the leg within this plane, the artifact band tilts as well (relative to the component), revealing more of the patella. The custom-built CT-compatible knee rig, in addition to raising the foot, loads the subject's knee as they resist a 9 kg weight by pushing on a pedal with their heel, thereby providing partial weight-bearing in the supine position (Fig. 2). We elected to use a fixed weight since using a percentage of maximal loading or percentage of body weight could lead to painful or difficult loading for some subjects.

Pre-TKA subjects undergo two sets of scans: hip, knee and ankle at 0° flexion (to obtain the HKA angle in addition to the knee parameters), and the knee alone at 30° flexion. Post-TKA subjects undergo three scans: hip, knee and ankle at 0° flexion with the foot lowered, knee at 0° flexion with the foot raised, and knee at 30° flexion with the foot raised. The 0° angle is at full extension; the 30° angle is measured with a goniometer. Subjects remove their shoes before imaging. Our institutional review board approved the subject imaging and informed consent was obtained from all subjects.

All imaging has been done on a clinical CT scanner (Somatom 64-slice, Siemens, Germany). Imaging parameters were selected to achieve good accuracy while keeping radiation dose low (Henckel et al., 2006; Van Sint Jan et al., 2006) (Table 1), with extended scale selected to avoid truncating the values at 3000 Hounsfield units. The metal artifact reduction algorithms built into the CT machine did not impact the image quality due to the large amount of metal in the femoral components. Density calibration phantoms are imaged for potential later use of the models in finite element analyses incorporating bone properties.

2.2. Image analysis

2.2.1. Analysis of preoperative geometry and pose

Pre-TKA CT images of the knee are autosegmented using an active shape model (ASM) algorithm that fits statistical shape models (SSM) of the femur, tibia and patella to a patient's 3D CT data (Seim et al., 2008). A statistical shape model consists of the mean of a complex shape together with its geometric shape variations, which are derived from a principal component analysis of a training set. In our case, the training set consisted of 90 femurs, 90 tibiae and 16 patellae, consisting of both healthy and arthritic bones. Fewer patellae were needed because the variations can be captured by fewer principle components. The ASM optimizes a linear combination of these shape modes to find the best fit to the patient data, including osteophytes that occur in typical locations. A subsequent automatic free-form segmentation allows for capturing small changes outside the possible variation of the SSM (Seim et al., 2008). Minimal manual correction is subsequently required to account for osteophytes not captured during the auto-segmentation due to their individual and localized nature. The autosegmentation

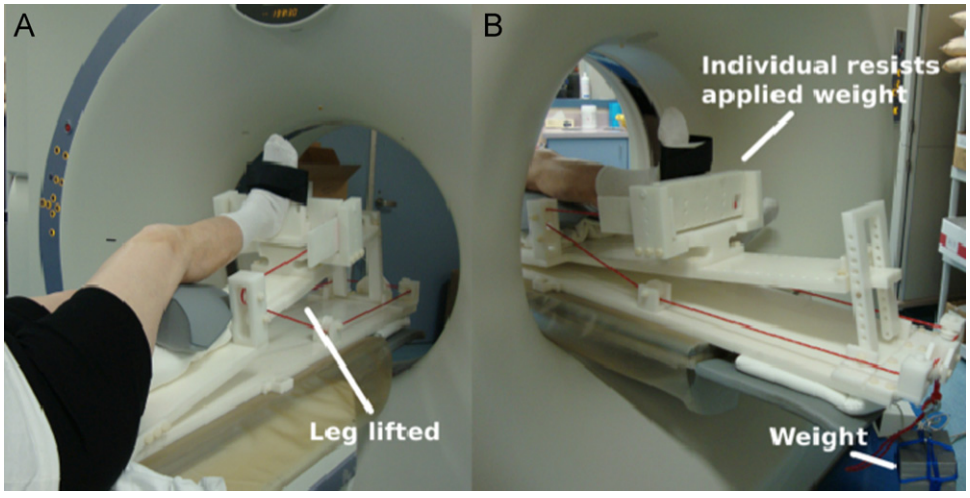

Fig. 2. (A) CT scanning setup at 30° knee flexion with leg lifted and partially loaded. (B) Knee rig partly loads the leg by applying weight to the foot through a pulley system.

Table 1
CT imaging parameters.

	FOV (mm)	kVp	Hip (cm)	Hip (mAs)	Knee (cm)	Knee (mAs)	Ankle (cm)	Ankle	Slice width (mm)	Slice thick (mm)
Preop	180	120	6	100	20	160	5	80	0.6	0.4
Postop	180	120	6	100	20	180	5	80	1.0	0.7

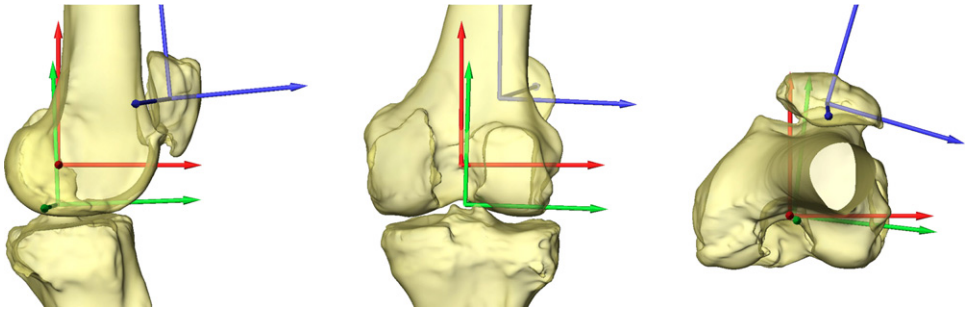

Fig. 3. Preoperative coordinate systems for the femur, tibia and patella.

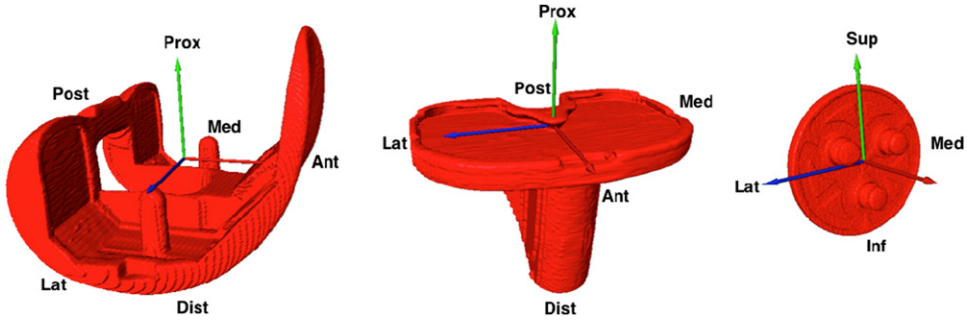

Fig. 4. Postoperative coordinate systems for the femoral, tibial and patellar components.

takes about 4 min, and can be run independently from the user; manual correction takes 10–15 min altogether for the three bones. 3D bone models are generated from the segmentations. If users of this protocol do not have access to a statistical shape model, the images can simply be manually segmented. The hip center is found automatically by fitting a sphere to the femoral head portion of the ASM. The ankle center is also found automatically, by calculating the point halfway between the malleoli landmarks.

Coordinate systems are computed automatically for the pre-TKA femur, tibia and patella 3D bone models at 0° knee flexion using anatomical features (Fig. 3). For the femur, spheres are fit to the medial and lateral condyles, and the centers joined to form the initial mediolateral (ML) axis (*z*-axis) (Iranpour et al., 2010). For further robustness, the diameters of the spheres are averaged and refit to the condyles, to avoid the effects of pathology and osteophytes. The origin is halfway between the condylar centers. The anteroposterior (AP) axis (*x*-axis) is the cross-product of the ML axis and the vector joining the knee and hip centers. The proximodistal (PD) axis (*y*-axis) is the cross-product of the other two axes to complete the system. The tibial frame is defined similarly: the ML axis joins the centers of the medial and lateral condyles (Cobb et al., 2008), defined by the center of mass of each surface, with the origin halfway between the tibial eminences. The AP axis is the cross-product of the ML axis and the vector joining the knee and ankle centers. The PD axis is the cross-product of the previous two axes. For the patella, the AP axis is defined perpendicular to the anterior surface; the ML axis is defined by the cross-product of the AP axis and the vector joining the geometric center and the inferior pole, and the PD axis is the cross-product of the other two axes. Once the coordinate systems are set, the 0° bone models are matched to the 30° femur, tibia, and patella 3D bone models, using an iterative surface align algorithm (ZIBAmira version 2011.2, Zuse Institute Berlin, Berlin). The resulting calculations provide the six DOFs of the PF and TF joints.

2.2.2. Analysis of postoperative geometry and pose

For the full post-TKA analysis, 3D implant models are required. These may be reverse engineered (via CT or laser scanning), or CAD models may be obtained from the manufacturer. We use the first option, reverse-engineering the components, using high-dose CT for the metal components and low-dose CT or microCT for the plastic components. Coordinate systems are assigned using prosthesis features, e.g. the vector joining the pegs defines the ML axis (Fig. 4). These prosthesis models are then fit to the CT scan of each subject using a 3D model-based reconstruction strategy, as follows. Knowing the prosthesis geometry, the reconstruction involves computing the rigid-body translations and rotations from model to image space by taking image gradient and gray value information into account with an optimization function. This technique is based on a rigid-body adaption of the approach used for statistical shape model fitting (Seim et al., 2008). To increase robustness and speed, the acceptable gradient magnitude and search space are progressively adapted during the optimization. This automated approach has many advantages; nevertheless, users of this protocol can fit the implants manually if necessary. The fitting takes approximately 10–15 s for each implant. The 6 DOF TF and PF relative poses are computed from the transformations of the tibial and patellar prosthesis coordinate systems relative to the femoral prosthesis coordinate frame.

2.2.3. Additional preoperative and postoperative analyses

Patellar Shift within the Groove: Most biomechanical studies only report the 6 DOF of the patellar bone or component with respect to the femoral bone or component. This does not provide information regarding how the patella is traveling within the femoral groove, which is of high clinical relevance since it determines whether the patella is tracking correctly or not. We analyzed this by taking a cross-section through the most prominent point (apex) on the posterior surface of the patella or patellar component and the epicondylar axis of the femur or the ML axis of the femoral component (Fig. 5, Ho, 2010). The epicondylar axis was used on the femur rather than the previously-defined ML axis as it was easier to locate on the defined slice and the difference had a negligible impact on the measurement of shift. The ML shift of the patella is then measured as the horizontal distance (medial or lateral offset) between the patellar apex and the visually deepest point of the femoral or femoral component groove.

Hip–Knee–Ankle (HKA) Angle: The 3D HKA angle is computed as the angle between the hip-to-knee center and the knee-to-ankle center vectors (see Section 2.2.1 and Figs. 3 and 4 for origin definitions). Although the whole leg is not imaged, the hip, knee and ankle are scanned in one sequence, and the relative positions of the hip, knee and ankle are therefore available in the CT coordinate system (Henckel et al., 2006).

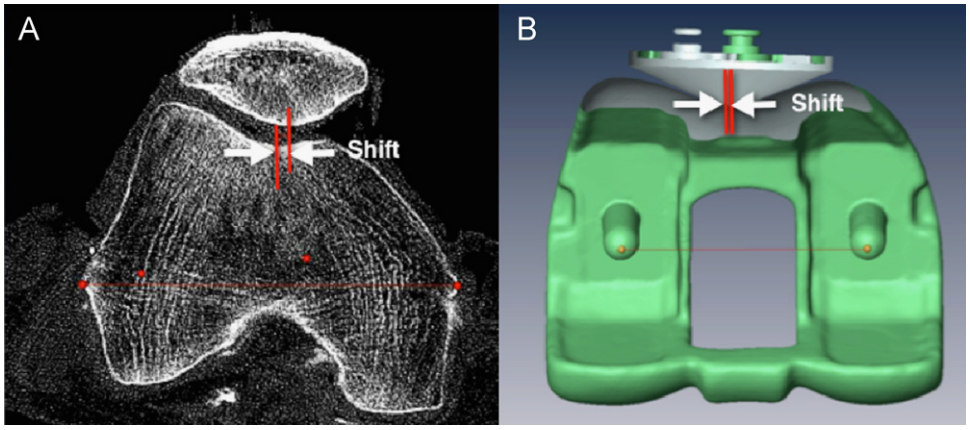

Fig. 5. (A) Preoperative patellar shift within the femoral groove. (B) Postoperative patellar component shift within the femoral component groove. The grey below the patella shows the cross-section through the femoral component in the plane of patellar contact.

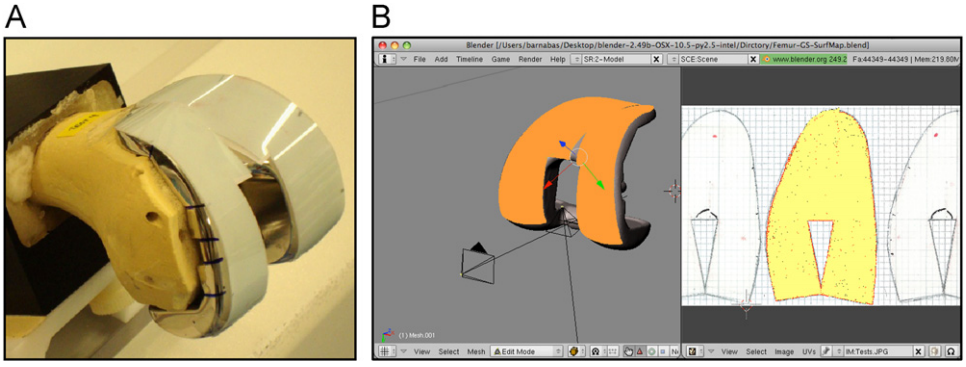

Fig. 6. (A) Fuji pressure-sensitive film overlaid on femoral component to validate PF and TF contact areas. (B) Using Blender software to overlay the digitally scanned marked film onto the 3D model of the prosthesis. The grid paper was used to remove distortions from the wrapping.

2.2.4. Additional postoperative analyses

Component Rotation: Malrotation of the femoral and tibial components can cause anterior knee pain and patellar maltracking. Our technique is based on previous work, with modifications to improve robustness (Amiri et al., in press).

PF and TF Contact Locations: Knowing the TF or PF implant contact location can indicate abnormal loading that could lead to component loosening or wear as well as functional limitations. PF and TF prosthesis contact locations are obtained by moving the patellar and tibial models towards the femoral model until there is a small amount of overlap between the models; the distance moved rarely surpasses 0.5 mm. The centroid of the intersecting area then defines the contact location.

Joint Line: Changes in the joint line (i.e. the proximodistal contact between the femur and tibia versus the femoral and tibial components) can affect knee stability, soft tissue laxity, range of motion and articular geometry. The current joint line height is defined by the PD distance from the medial and lateral condyles to the surgical transepicondylar axis (TEA) on a slice passing through the center of the femoral pegs. This is compared to the regression equation for the original height: length_of_TEA/3.2 (Mountney et al., 2007) to determine the change in joint line.

Patellar Cut Symmetry, *Patellar Thickness and Patellar Height:* Asymmetry of the patellar cut can result in anterior knee pain, bony impingement, patellar maltracking, and component loosening. This angle can be measured by comparing a plane fit automatically to the resection surface (which has not been done previously) versus the anterior surface, as the resection goal is to be parallel to the anterior surface (Anglin et al., 2009). Patellar thickness is the maximum depth in the AP direction. Patellar height, which can impact patellar tracking, anterior knee pain, bony impingement and soft tissue balancing, is determined from the Insall–Salvati ratio, (patellar tendon length)/(patellar bone length), where the normal ratio is 1.02 (Sasaki et al., 2011).

2.3. Accuracy and repeatability

Validation of Knee Pose: For validation, femoral, tibial and patellar prostheses were implanted onto an artificial bone model that was fixed in place and then CT scanned using our normal protocol. The implants were then digitized using a coordinate measuring machine (CMM) (FaroArm, FARO Technologies, Lake Mary, FL; accuracy 0.025 mm) at key points and with a point cloud covering the surface. The 3D implant models were fit to the combined point cloud data to determine the CMM-based 6 DOF TF and PF; this was compared to the CT-based results using our normal protocol. There was no noticeable difference in fitting the femoral and tibial prostheses to the in vivo data and the Sawbones data; whether in the artificial or in vivo case, the main barrier is still the metal artifact band. The patellar component did have better contrast to the artificial bone, but it is unlikely this affected the robustness of the results.

Validation of Contact Locations: Contact locations were validated by comparing the CT imaging results to the marks left on pressure-sensitive film (Fujifilm Holdings, Tokyo, Japan) mounted on prosthesis components implanted onto loaded artificial bone models at 0° and 30°, with the patella aligned in the femoral groove, and offset by 5 mm. The films were shaped and carefully overlaid on the prosthesis models in a repeatable manner (Fig. 6a). The marked films were scanned into the computer and virtually overlaid onto the prosthesis surface using Blender software (V2.4.9; Stichting Blender Foundation, Amsterdam, Netherlands, Fig. 6b). The contact areas from the CT and Fuji scans were compared directly by applying the same transformation matrix used to register the model to the CT scans to the STL prosthesis models in Blender. Distortions were corrected by comparing the digitally wrapped scan of square grid paper to a computer-generated grid of the same dimensions. Contact location was defined as the centroid of the mark left on the film.

Repeatability and Robustness of Knee Pose: The implant matching algorithm, which is an important advance over the manual method we developed initially (Ho, 2010), was tested for repeatability and robustness on in vivo images by adjusting ten parameters (four related to fitting, six related to the initial position of the implant), alone and in combination, for a total of 15,049 parameter sets for the femoral component, 23,000 for the tibial component, and 13,865 for the patellar component, varying initial position by ± 5 mm, initial orientation by $\pm 10^{\circ}$, and four fitting parameters to determine confidence intervals and error estimates for the implant fitting.

2.4. Radiation dose and subjects

Radiation Dose: The total effective radiation dose for the protocol is approximately 2.2 mSv for preop subjects and 2.5 mSv for postop patients, with the largest contribution (1.4 mSv) coming from the hip scan. This is less than the 3 mSv for

average yearly background radiation and considerably less than the 7 mSv for a standard chest CT (Mettler et al., 2008). Older individuals, who make up most of the TKA population, are at a much lower risk from radiation.

Subjects: We have used this procedure in vivo on numerous subjects with different implant designs, with and without pain, to address various research questions.

3. Results

Sample preoperative and postoperative knee pose and geometry at 0° and 30° are shown in Figs. 7 and 8, showing the sequence of steps in the image analysis. Data are also available for the clinical measures described above.

Validation showed highly comparable CT and CMM translations and rotations, with maximum TF and PF translational differences <0.5 mm and <0.4 mm respectively and TF and PF rotational differences $<0.7°$ and $<0.3°$ respectively (excluding patellar spin, since the patellar pegs were not digitized, Table 2). Mean absolute differences were: 0.24 mm TF, 0.19 mm PF, 0.40° TF, and 0.22° PF. Contact location validation demonstrated

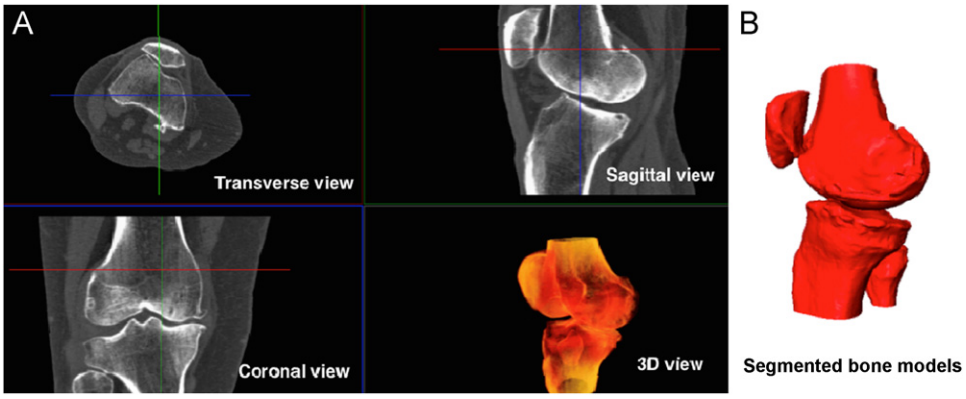

Fig. 7. Preoperative images: (A) original CT image at 0°, (B) segmented bones at 0°.

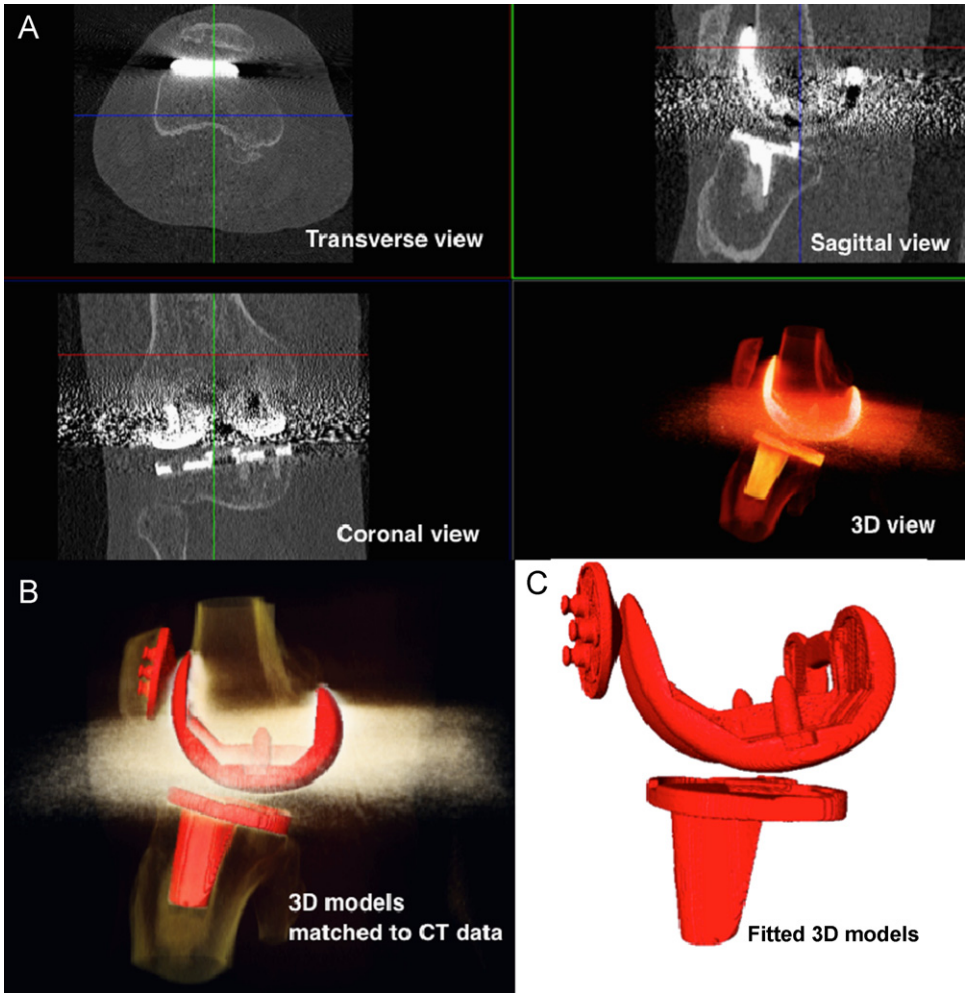

Fig. 8. Postoperative images: (A) original CT image at 0°, (B) prosthesis pose and geometry at 0°, overlayed on CT image, (C) fitted models showing relative pose of implants.

Table 2
Accuracy of CT pose compared to coordinate measuring machine digitized pose.

	Tibial translation (mm)			Tibial rotation (°)			Patellar translation (mm)			Patellar rotation (°)		
	ant/pos	sup/inf	lat/med	var/val	int/ext	ext/flx	ant/pos	sup/inf	lat/med	ex/in spin	ML tilt	ext/flx
CMM	−21.08	−25.80	−2.10	−1.73	14.26	−36.07	33.27	−6.09	3.32	–	1.44	−17.63
CT	−20.62	−26.04	−2.07	−1.95	13.99	−35.37	33.23	−5.74	3.50	–	1.25	−17.87
Diff	−0.46	0.24	−0.03	0.22	0.27	−0.70	0.04	−0.35	−0.18	–	0.19	0.24

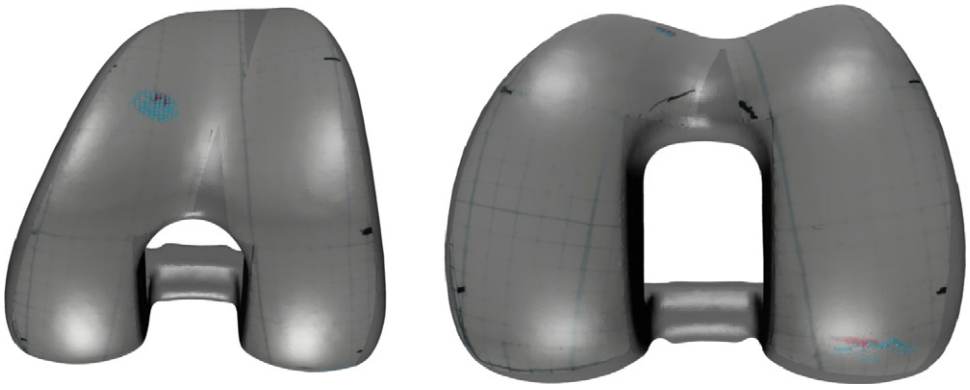

Fig. 9. Comparison of CT contact (blue) and pressure-sensitive film contact (red). In this example, the patella is in its shifted (maltracking) position and the joint is in higher flexion. Contact only occurred on one condyle due to a loading imbalance, which was seen in both the CT and Fuji film results, confirming the validation. (For interpretation of the references to color in this figure legend, the reader is referred to the web version of this article.)

PF differences of 1.48 ± 0.65 mm and TF differences of 2.00 ± 0.87 mm between the CT and Fuji-film locations (Fig. 9).

Repeatability of the 3D–3D matching procedure showed standard deviations (SD) of 0.29° or less in rotation for all components and 0.11 mm or less in translation for all components. The optimized position was robust to a large range of input parameters: the femoral and tibial implant could be positioned anywhere within 4 mm and 9° (femur) or 10° (tibia) of the highest-density point and achieve the desired position within the given standard deviation; this is easy for the user to achieve as it is clear at these limits that the implant is mismatched. The patellar component position needs to be positioned slightly more precisely, within 3 mm in AP and ML position, within 1 mm PD, and within 8° in rotation, to achieve these SDs. This automated implant matching is considerably more repeatable and faster than the original manual method, which had intra-observer RMS errors of 0.76° and 0.48 mm and inter-observer RMS errors of 1.36° and 0.83 mm (Ho, 2010).

4. Discussion

A clinical CT imaging protocol to measure knee pose and geometry before and after TKA was successfully developed and validated. Despite the metal artifact in post-TKA CT images, our technique of raising the individual's leg was able to reveal the majority of the patellar prosthesis, especially its fixations. The method demonstrates excellent accuracy and repeatability.

To our knowledge, this is the first time that patellofemoral pose and geometry have been analyzed using CT, pre-or post-TKA. It is also the first time that we are of aware of that 3D implant models have been fit automatically to CT images, or that post-operative contact locations have been determined from CT; the contact validation procedure of wrapping the film virtually onto the femoral component is also novel to our knowledge. Not only is the automated procedure more repeatable, but it can be completed in a fraction of the time; all that is required of the user is to position the implants in their approximate location and start the script routine. This could be a valuable option for checking the accuracy of component placement after the use of custom surgical guides or computer-assisted surgery. The automated 3D–3D matching procedure was made possible by applying techniques from the image analysis domain to orthopaedic biomechanics, with unique developments to recognize and ignore the metal artifact regions. Increasingly powerful and efficient computers continually decrease the processing time required.

MRI has been used to assess knee pose parameters (Carpenter et al., 2009), however disadvantages exist to using MRI: metal prostheses create artifacts and unknown distortions in MRI, particularly for non-titanium implants such as the cobalt-chrome femoral component used in our study; low-field MRI produces poor bone boundary definition; resolution is lower than in CT, and subjects must remain stationary for a considerable time. MRI is also more costly and less available than CT.

The main limitations of our method are that only low knee flexion can be achieved and the leg is only partially loaded. Nevertheless, low flexion angles are sufficient to retrieve the bone and implant geometries, which can be used to differentiate between patients with and without postoperative problems, e.g. due to component malrotation, as well as bone or implant pose. These results can be combined with quality-of-life questionnaires, clinical data and physiotherapy measures such as range of motion. If only the geometry is needed (e.g. the shapes of the bones or bone plus prosthesis) or the positioning of the implant relative to the bone (e.g. to indicate malrotation), and not the pose of the bones or prostheses relative to each other under physiological loading (e.g. to indicate patellar maltracking), then the knee rig that partially loads the leg is not required, making this protocol easy to adopt at any hospital. Also, depending on the research question or clinical question, it may not be necessary to scan the subject's knee at both 0° and 30°, resulting in a simpler diagnostic tool.

The 3D bone and implant models derived from this method can be used for other purposes as well. Combining the CT results with

fluoroscopy or radiography can provide subject data throughout a large range of motion (Sharma et al., 2012). Furthermore, the models can be used for finite element analyses related to implant design and positioning, joint biomechanics, or SPECT-CT (Hirschmann et al., 2010).

The presented tools allow us to investigate the causes of post-TKA problems, particularly related to the PF joint, including determining changes in the joint due to arthroplasty, differences related to implant design or surgical technique, changes over time postoperatively, and differences between patients with and without pain. The automated analysis techniques make this approach suitable for widespread clinical use.

Conflict of interest statement

Funding was provided by the Natural Sciences and Engineering Research Council of Canada (NSERC), Canadian Institutes for Health Research (CIHR), Alberta Innovates – Technology Futures (AITF), and the University of Calgary. The authors have no other conflicts of interest. The study sponsors had no involvement in the study or manuscript preparation.

Acknowledgments

The development of this protocol was a large undertaking, with valuable contributions from many individuals. We would like to thank Deb Iampen, Roy Pooley and the CT technologists for helping us develop the protocols and acquire the images; John Kornelson and Calvin Cockerline for their support in the Anatomy lab; Agnes d'Entremont and Emily McWalter for their advice on the knee rig; Carolina Romeo for her work on the original knee rig; Sara Emslie, Eva Szabo, Michelle Kan and Steve Boyd for their assistance with scanning the implants; Dr. Leszek Hahn for his input regarding the radiation dose calculations; and Dr. Richard Frayne, Dr. Janet Ronsky, Dr. Carol Hutchison and Dr. David Wilson for their technical and clinical advice. We gratefully acknowledge funding provided by the Natural Sciences and Engineering Research Council of Canada (NSERC), Canadian Institutes for Health Research (CIHR), Alberta Innovates – Technology Futures (AITF) and the University of Calgary.

References

Anglin, C., Fu, C., Hodgson, A.J., Helmy, N., Greidanus, N.V., Masri, B.A., et al., 2009. Finding and defining the ideal patellar resection plane in total knee arthroplasty. Journal of Biomechanics 42, 2307–2312.

Amiri, S., Wilson, D.R., Vanhouwelingen, A., Anglin, C., Masri, B.A. Isocentric 3D C-arm imaging of component alignments in total knee arthroplasty with potential intraoperative and postoperative applications. Journal of Arthroplasty (in press).

Carpenter, R.D., Brilhault, J., Majumdar, S., Ries, M.D., 2009. Magnetic resonance imaging of in vivo patellofemoral kinematics after total knee arthroplasty. The Knee 16, 332–336.

Cobb, J.P., Dixon, H., Dandachli, W., Iranpour, F., 2008. The anatomical tibial axis: reliable rotational orientation in knee replacement. Journal of Bone and Joint Surgery, British Volume 90, 1032–1038.

DeFrances, C.J., Cullen, K.A., Kozak, L.J., 2007. National hospital discharge survey: 2005 annual summary with detailed diagnosis and procedure data. Vital and Health Statistics. Series 13, Data from the National Health Survey 165, 1–209.

Henckel, J., Richards, R., Lozhkin, K., Harris, S., Baena, F.M., Barrett, A.R., Cobb, J.P., 2006. Very low-dose computed tomography for planning and outcome measurement in knee replacement. The Imperial knee protocol. Journal of Bone and Joint Surgery British Volume 88, 1513–1518.

Hirschmann, M.T., Iranpour, F., Konala, P., Kerner, A., Rasch, H., Cobb, J.P., Friederich, N.F., 2010. A novel standardized algorithm for evaluating patients with painful total knee arthroplasty using combined single photon emission tomography and conventional computerized tomography. Knee Surgery, Sports Traumatology, Arthroscopy 18, 939–944.

Ho, K.C.T., 2010. Computed Tomography Protocol For Measuring Knee Kinematics Before and After Total Knee Arthroplasty. M.Sc. Thesis, University of Calgary.

Iranpour, F., Merican, A.M., Dandachli, W., Amis, A.A., Cobb, J.P., 2010. The geometry of the trochlear groove. Clinical Orthopaedics and Related Research 468, 782–788.

Mettler Jr., F.A., Huda, W., Yoshizumi, T.T., Mahesh, M., 2008. Effective doses in radiology and diagnostic nuclear medicine: a catalog. Radiology 248, 254–263.

Mountney, J., Karamfiles, R., Breidahl, W., Farrugia, M., Sikorski, J.M., 2007. The position of the joint line in relation to the trans-epicondylar axis of the knee: complementary radiologic and computer-based studies. Journal of Arthroplasty 22, 1201–1207.

Sasaki, H., Kubo, S., Matsumoto, T., Muratsu, H., Matsushita, T., Ishida, K., Takayama, K., Oka, S., Kurosaka, M., Kuroda, R., 2011. The influence of patella height on intra-operative soft tissue balance in posterior-stabilized total knee arthroplasty. Knee Surgery, Sports Traumatology, Arthroscopy. (Epub ahead of print).

Seim, H., Kainmueller, D., Heller, M., Lamecker, H., Zachow, S., Hege, H.C., 2008. Automatic segmentation of the pelvic bones from CT data based on a statistical shape model. In: Botha, C.P., Kindlmann, G., Niessen, W.J., Preim, B. (Eds.), Eurographics Workshop on Visual Computing for Biomedicine.

Sharma, G.B., Saevarsson, S.K., Amiri, S., Montgomery, S., Ramm, H., Lichti, D.D., Zachow, S., Anglin, C., 2012. Sequential-biplane radiography for measuring pre and post total knee arthroplasty kinematics. Orthopaedic Research Society Annual Meeting. San Francisco.

Van Sint Jan, S., Sobzack, S., Dugailly, P.M., Feipel, V., Lefevre, P., Lufimpadio, J.L., Salvia, P., Viceconti, M., Rooze, M., 2006. Low-dose computed tomography: a solution for in vivo medical imaging and accurate patient-specific 3D bone modeling? Clinical Biomechanics 21, 992–998.